

Article

**Sliced Magnetic Polyacrylamide Hydrogel with Cell-Adhesive
Microarray Interface: A Novel Multicellular Spheroid Culturing Platform**Ke Hu, Naizhen Zhou, Yang Li, Siyu Ma, Zhaobin Guo, Meng
Cao, Qiyong Zhang, Jianfei Sun, Tianzhu Zhang, and Ning GuACS Appl. Mater. Interfaces, **Just Accepted Manuscript** • DOI: 10.1021/acsami.6b04112 • Publication Date (Web): 03 Jun 2016Downloaded from <http://pubs.acs.org> on June 8, 2016**Just Accepted**

“Just Accepted” manuscripts have been peer-reviewed and accepted for publication. They are posted online prior to technical editing, formatting for publication and author proofing. The American Chemical Society provides “Just Accepted” as a free service to the research community to expedite the dissemination of scientific material as soon as possible after acceptance. “Just Accepted” manuscripts appear in full in PDF format accompanied by an HTML abstract. “Just Accepted” manuscripts have been fully peer reviewed, but should not be considered the official version of record. They are accessible to all readers and citable by the Digital Object Identifier (DOI®). “Just Accepted” is an optional service offered to authors. Therefore, the “Just Accepted” Web site may not include all articles that will be published in the journal. After a manuscript is technically edited and formatted, it will be removed from the “Just Accepted” Web site and published as an ASAP article. Note that technical editing may introduce minor changes to the manuscript text and/or graphics which could affect content, and all legal disclaimers and ethical guidelines that apply to the journal pertain. ACS cannot be held responsible for errors or consequences arising from the use of information contained in these “Just Accepted” manuscripts.

Sliced Magnetic Polyacrylamide Hydrogel with Cell-Adhesive Microarray

Interface: a Novel Multicellular Spheroid Culturing Platform

Ke Hu¹†, Naizhen Zhou¹†, Yang Li¹, Siyu Ma¹, Zhaobin Guo¹, Meng Cao¹, Qiyong Zhang¹, Jianfei Sun^{1,2}, Tianzhu Zhang^{1,2*}, and Ning Gu^{1,2*}

¹ State Key Laboratory of Bioelectronics, Jiangsu Laboratory for Biomaterials and Devices, School of Biological Sciences and Medical Engineering, Southeast University, Nanjing, China

² Collaborative Innovation Center of Suzhou Nano-Science and Technology, Suzhou Key Laboratory of Biomaterials and Technologies, Suzhou, 215123, China

ABSTRACT

Cell-adhesive properties are of great significance to materials served as extracellular matrix mimics. Appropriate cell-adhesive property of material interface can balance the cell-matrix interaction and cell-cell interaction and promote cells to form three-dimensional structures. Herein, a novel magnetic polyacrylamide (PAM) hydrogel fabricated *via* combining magnetostatic field induced magnetic nanoparticles assembly and hydrogel gelation was applied as a multicellular spheroids culturing platform. When cultured on the cell-adhesive microarray interface of sliced magnetic hydrogel, normal and tumor cells from different cell lines could rapidly form multicellular spheroids spontaneously. Furthermore, cells which could only form loose cell aggregates in classic 3D cell culture model (such as hanging drop system) were able to be promoted to form multicellular spheroids on this platform. In the light

1
2
3
4 of its simplicity in fabricating as well as effectiveness in promoting formation of
5
6 multicellular spheroids which was considered as a prevailing tool in the study of the
7
8 microenvironmental regulation of tumor cell physiology and therapeutic problems,
9
10 this composite material holds promise in anti-cancer drugs or hyperthermia therapies
11
12 evaluation *in vitro* in the future.
13
14
15
16
17
18

19 KEYWORDS: magnetic hydrogel, cell-adhesive microarray interface, cell-matrix
20
21 interaction, cell-cell interaction, multicellular spheroids, 3D cell culture
22
23
24
25

26 1. INTRODUCTION

27

28
29 Hitherto, monolayer cell culture model has provided many important results to
30
31 interpret biological phenomena. However, researches show that cell behaviors are
32
33 often unnatural when excised from native three dimensional (3D) tissues and cultured
34
35 on cell culture plates or Petri dishes^{1,2}. Findings in stem cell differentiation elucidate
36
37 acute disparities in cell functions between 2D and 3D cell culture³. Tumor cells
38
39 culture in 2D plate also display lower resistance to radiotherapy and chemotherapy
40
41 compared with tumor cells *in vivo*⁴. These deficiencies of traditional 2D culture
42
43 models lead growing numbers of researchers switch to develop novel materials for
44
45 developing synthetic extracellular matrix (ECM) analogs⁵⁻⁹. These matrices are
46
47 designed based on one or more structural or functional features of ECM to promote
48
49 cells to form 3D structures¹⁰. Multicellular spheroid, an important *in vitro* 3D model
50
51 for both stem and tumor cell research, is usually generated by preventing cells
52
53
54
55
56
57
58
59
60

1
2
3
4 adherent to matrix therefore favoring cell-cell interaction¹¹. Most matrices developed
5
6 for generating multicellular spheroids were focused vitally on the anti-cell adhesive
7
8 interfacial properties^{12,13}.
9

10
11 The degree and distribution of cell adhesive sites on the interface of matrix will
12
13 greatly affect the cell behavior. Recent studies have indicated that a strong cell-matrix
14
15 interaction between cells and 2D substrates induces cellular features that differ from
16
17 those growing *in vivo*¹⁴. It might be due to the competition between cell-cell and
18
19 cell-matrix interaction which is greatly affected by the cell adhesive environment^{15,16}.
20
21

22
23 We believe it's essential to balance cell-cell and cell-matrix interaction by controlling
24
25 the interfacial adhesion properties for mimicking the ECM to build *in vitro* culture
26
27 models. Researchers also found that multicellular hepatocyte spheroids could be
28
29 formed when cultured in different natural materials by controlling the cell adhesive
30
31 properties¹⁷.
32
33

34
35 Due to their ability to simulate the nature of most soft tissues, hydrogels capture
36
37 numerous characteristics of the architecture and mechanics of the native cellular
38
39 microenvironment. Recently, applying hydrogel-based composite materials as cell
40
41 culture matrices draws the attention of many researches. Among the diverse
42
43 preparation strategies, the combination of nanomaterial and hydrogel holds promise of
44
45 providing superior functionality^{18,19}. Interfacial properties of materials for cell culture
46
47 have been implicated to play increasingly important roles on a wide spectrum of
48
49 cellular functions²⁰. The heterogeneous interface of nanomaterial-hydrogel composite
50
51 could affect cell behaviors and mimic ECM to a certain extent.
52
53
54
55
56
57
58
59
60

1
2
3
4 In our previous work, we have fabricated a novel magnetic hydrogel with anisotropic
5
6 properties and controllable enhancement of magnetothermal effect when placing in
7
8 the alternating magnetic field²¹. In this study, we applied the slice of this
9
10 multifunctional magnetic hydrogel as 3D cell culture matrix. Cell adhesive assemblies
11
12 array combined with anti-cell adhesive substrate enhance the cell-cell interaction and
13
14 promote the spontaneous formation of multicellular spheroid by both epithelial and
15
16 cancer cells (Figure 1). This composite material could provide a new platform for
17
18 different applications such as anticancer drugs or hyperthermia therapies models *in*
19
20
21
22
23
24 *vitro*.

25 26 27 28 29 2. MATERIALS AND METHODS

30 31 32 33 2.1 Materials

34
35
36 Polyglucose sorbitol carboxymethylether encapsulated Fe₃O₄ magnetic nanoparticles
37
38 (Fe₃O₄@PSC MNPs) were provided by Jiangsu Key Laboratory for Biomaterials and
39
40 Devices. Millipore-quality water (18.25 MΩcm⁻¹), prepared with a Milli-Q Plus water
41
42 system, was the only used water throughout experiments. Human embryonic kidney
43
44 293A (stably transfected with enhanced green fluorescent protein encoding gene
45
46 (EGFP)) were established and provided by Jiangsu Key Laboratory for Biomaterials
47
48 and Devices. Breast cancer cell line MCF-7 and ovarian cancer cell line SK-OV-3
49
50 were purchased from Chinese Academy of Science Shanghai cell bank. Unless stated,
51
52
53
54
55
56
57
58
59
60 all reagents were purchased from Aladdin Industrial Inc.

2.2 Preparation of sliced magnetic hydrogel

The preparation of anisotropic magnetic hydrogel has been described previously¹⁸. Briefly, Fe₃O₄@PSC MNPs, acrylamide monomer (87 mg), N,N'-methylene-bis-acrylamide (9 mg), ammonium persulfate (2.4 mg), and tetraethylethylenediamine (0.2 μL) were mixed in 1 mL water first. The mixed solution was poured into a PTFE module after ultrasonic agitation for 10 min and then subjected to a magnetostatic field. After a certain time for assembling, the gelation of PAM was triggered by heating with a ceramic heating flake to 50 °C. The disorganized magnetic hydrogel was fabricated as the same procedure but in absence of magnetic field. Then the obtained magnetic PAM hydrogel was fixed in an aluminum mould and sliced with a low profile microtome blade. The final size of sliced magnetic hydrogel for 3D cell culture was 0.2 × 1.0 × 1.0 cm³. Before the biological experiments, the magnetic hydrogel was dialyzed for 2 days.

2.3 Morphology characterization of sliced magnetic hydrogel

Optical microscope images of sliced magnetic hydrogel and fluorescence microscope images were taken with a BX63 Olympus microscope. The optical microscope images were transferred into binary images with ImageJ and the section areas of assemblies and interval between magnetic nanoparticle assemblies was measured based on these binary images with ImageJ. Atomic force microscopy (AFM) images were taken with a Bruker Dimension FastScan Atomic force microscope. The sample was firstly

1
2
3 replicated with polydimethylsiloxane (PDMS) then scanned with AFM.
4
5
6
7

8 9 2.4 Cell culture

10
11 Sliced magnetic hydrogel first was rinsed with PBS twice, then sterilized by
12
13 immersed in ethanol solution (75%) for 24 hour and in PBS for 24 hour. Then the
14
15 slice magnetic hydrogel was incubated with cell culture medium for 12 hour before
16
17 cell culturing. GFP-293A, MCF-7 and SK-OV-3 cells (1×10^6 cells/mL, 15 μ L) in
18
19 single cell suspension were grown on sliced magnetic hydrogel placed in 24 well
20
21 cell-culture plates. Following initial plating of cells, they were allowed to adhere to
22
23 the hydrogel before addition of complete growth medium to 3 mL. All cultures were
24
25 maintained in an incubator at 37 °C in an atmosphere of 5% CO₂. Live/dead cells
26
27 were stained with Fluorescein diacetate (FDA)/Propidium Iodide (PI) dye. Cell
28
29 viability of tumor cells (SK-OV-3) cultured on cell culture plates and sliced magnetic
30
31 hydrogel were characterized with cell counting kit-8 (CCK-8).
32
33
34
35
36
37
38
39
40

41 2.5 Time lapse-microscopy

42
43 Time-lapse images of cells seeded on sliced magnetic hydrogel were acquired every
44
45 20 min at 100 \times magnification for 1 day using an X-living cell workstation
46
47 (Olympus).
48
49
50
51
52

53 2.6 Laser confocal fluorescence microscopy

54
55 Laser confocal fluorescence images were acquired at 100 \times magnification using a SP8
56
57
58
59
60

1
2
3
4 (Leica) laser confocal fluorescence microscopy.
5
6
7

8 9 2.7 Drug cytotoxicity analysis

10
11 To establish dose response of cells on monolayer and sliced magnetic hydrogel, cells
12
13 were treated with 2, 25 and 100 $\mu\text{g/mL}$ doxorubicin in standard medium after a given
14
15 culture period. Cytotoxicity was evaluated following a 24-hour incubation on both
16
17 monolayer and sliced magnetic hydrogel.
18
19
20
21
22

23 24 3. RESULTS AND DISCUSSION

25 26 27 28 29 3.1 Fabrication and characterization of sliced magnetic hydrogel

30
31 In our experiments, owing to good biocompatibility and magnetism, Fe_3O_4
32
33 nanoparticles coated by polyglucose sorbitol carboxymethyether ($\text{Fe}_3\text{O}_4@\text{PSC}$) were
34
35 used as the building block (Supporting Information Figure s1)²². The average
36
37 hydrodynamic diameter of $\text{Fe}_3\text{O}_4@\text{PSC}$ nanoparticles was 201 nm and the magnetic
38
39 force on this nanomaterial can effectively overwhelm the thermal perturbation based
40
41 on our calculation¹⁸. PAM hydrogel was chosen as host material because it is
42
43 biocompatible after dialysis and the mechanical property of hydrogel is suitable as
44
45 mimic for ECM¹⁴. By combining static magnetic field-assisted assembly of magnetic
46
47 nanoparticles and gelation together, we fabricated this magnetic hydrogel with
48
49 anisotropic properties. Since the assemblies were encapsulated inside the hydrogel,
50
51 magnetic hydrogels were sliced in order to expose assemblies on the interface.
52
53
54
55
56
57
58
59
60

1
2
3
4 Sample (1.0 cm × 1.0 cm × 1.0 cm) was fixed in a mould to avoid break caused by
5
6 deformation of anisotropic hydrogel when slicing and sliced with a low profile
7
8 microtome blade. The final size of sliced magnetic hydrogel for 3D cell culture was
9
10 0.2 cm × 1.0 cm × 1.0 cm.
11

12
13 A series of sliced magnetic with different concentration of Fe₃O₄ nanoparticles (0.05
14
15 mg/mL, 0.3 mg/mL and 1.8 mg/mL, respectively) were fabricated and labeled as
16
17 SMH-1, SMH-2 and SMH-3. The increase of concentration of Fe₃O₄ nanoparticles
18
19 could be easily distinguished with naked eyes (Figure 2a) and the optical microscope
20
21 images of side view of sliced magnetic hydrogel accorded with this tendency
22
23 (Supporting Information Figure s2). The section morphologies of sliced magnetic
24
25 hydrogel with Fe₃O₄ nanoparticles as building block are characterized with optical
26
27 microscope (Figure 2b). Previous studies showed that assembly process could
28
29 promote the homogeneity of the distribution of nanomaterials inside the hydrogel²³.
30
31 The optical microscope images of sliced magnetic hydrogels were analyzed with
32
33 image processing software. Specifically, sectional areas of and intervals between
34
35 assemblies were measured and percentage of assemblies in the section area of sliced
36
37 magnetic hydrogel was calculated. Results demonstrated that structure properties of
38
39 assemblies array (assemblies' number and sectional areas) on the surface were of no
40
41 significant difference between each sample with different slicing depth and showed a
42
43 good reproducibility (Supporting Information Figure s3). As in Figure 3, the area of
44
45 one assembly, which largely distributed around 4-12 μm², is growing slightly when
46
47 the concentration of nanoparticles increased. According to Figure 3a, the peak value
48
49
50
51
52
53
54
55
56
57
58
59
60

1
2
3 emerges at area of $4 \mu\text{m}^2$, $8 \mu\text{m}^2$ and $12 \mu\text{m}^2$ in SMH-1, SMH-2, and SMH-3,
4
5
6 respectively. At lower nanoparticle concentration (SMH-1 and SMH-2), the ratio of
7
8 assemblies in area ranging from 4 to $8 \mu\text{m}^2$ is near to 90% while at higher
9
10 concentration more than 60% of assemblies are in range of $8\text{-}12 \mu\text{m}^2$. Furthermore, as
11
12 showed in Figure 3b, the concentration impacts the interval between assemblies
13
14 significantly. The distribution of interval of SMH-1 is quite wide, from 10 to 40 μm .
15
16 With the concentration increasing, the distribution become narrower and the interval
17
18 between assemblies of SMH-3 is only ranging from 5-10 μm , which showed that with
19
20 the increasing of concentration the degree of homogeneity of assemblies also
21
22 improved.
23
24
25
26
27
28
29
30

31 3.2 Sliced magnetic hydrogel applied as 3D cell culture matrix

32
33 Previous studies showed that cell-cell interaction played an important role in cell
34
35 behaviors and functions²³. Strong cell-matrix interaction inhibited the formation of
36
37 cell-cell interaction when cells were cultured on 2D plates. Based on this, researchers
38
39 fabricated hydrogels and electro spinning scaffolds with limited cell-adhesive sites to
40
41 promote the cell-cell interaction and several cancer cell lines were able to form
42
43 multicellular spheroids when cultured on these matrices^{25,26}. Sliced magnetic hydrogel
44
45 composed by cell-adhesive nanoparticle assemblies and anti cell-adhesive hydrogel
46
47 also capable of providing a matrix with cell adhesive properties more possibly accord
48
49 with the ECM than the traditional monolayer culture plate. Since cells can not adhere
50
51 on the hydrophilic surface of the PAM hydrogel, the cell adhesive function of
52
53
54
55
56
57
58
59
60

1
2
3
4 magnetic hydrogel are provided by the magnetic nanomaterials. However, we found
5
6 that very few cells could adhere on the surface of disorganized sliced magnetic
7
8 hydrogel which was fabricated in absence of magnetic field (Supporting Information
9
10 Figure s4). This might because that the array consisted of randomly distributed
11
12 magnetic nanoparticles were too small to support cells to form focal adhesion²⁷.
13
14 Compared to the unassembled magnetic nanoparticles, the sectional area of magnetic
15
16 colloidal assemblies were large enough for single cell to form focal adhesion.
17
18 Moreover, magnetic nanoparticles of the colloidal assemblies were less likely to be
19
20 encapsulated inside the hydrogel after slicing. Since the magnetic hydrogels were
21
22 sliced before being applied as cell culture matrix, the roughness of sliced surface was
23
24 characterized by atomic force microscope in area of $400 \mu\text{m}^2$ ($20 \mu\text{m} \times 20 \mu\text{m}$) which
25
26 is close to the area of one single cell after moulding with polydimethylsiloxane
27
28 (PDMS) (Supporting Information Figure s5). Generally, the height of the peaks and
29
30 valleys were ranging from tens to hundreds of nanometers, while specifically the
31
32 surface roughness (Ra) is $422 \pm 169 \text{ nm}$, which quite close to a polished surface²⁷.
33
34 Research showed that surface roughness ranged from $1 \mu\text{m}$ to tens of micron would
35
36 affect the behavior of cells²⁹. The roughness of magnetic hydrogel caused by slicing
37
38 was out of this range (both larger and smaller than) and had little impacts on cells.
39
40 Consequently, we believe the sliced surface of magnetic hydrogel could be regarded
41
42 as smooth surface to cells³⁰.
43
44
45
46
47
48
49
50
51
52

53
54 To evaluate the performance of sliced magnetic hydrogel as 3D cell culture platform,
55
56 human embryonic kidney 293A (stably transfected with enhanced green fluorescent
57
58
59
60

1
2
3
4 protein encoding gene (EGFP)) was chosen because 293A cells tended to form
5
6 multicellular spheroid in traditional non-adhesive 3D culture model. A GFP-293A
7
8 single cell suspension (15 μL of 1×10^6 cells/mL) was pipetted onto the surface of
9
10 the composite material placed in a 24 well plate. After 1 hour incubation in CO_2
11
12 incubator, 3 mL culture medium was added. According to the optical microscope
13
14 images, the proportion of cell adhesive sites areas on the surface of sliced magnetic
15
16 hydrogel were rose with increasing concentration of magnetic nanoparticles. Sliced
17
18 magnetic hydrogels with concentration of Fe_3O_4 nanoparticles higher than 0.3 mg/mL
19
20 were light-tight and morphology of cells cultured on these composite materials could
21
22 hardly be observed with inverted microscope. So the cell cultured on sliced magnetic
23
24 hydrogel with concentration of Fe_3O_4 nanoparticles higher than 0.4 mg/mL was
25
26 observed after the composite material was overturned. After preliminary experiments
27
28 we found that GFP-293A cells cultured on all of three samples with different density
29
30 of cell-adhesion sites could form multicellular spheroids after 6 days (Supporting
31
32 Information Figure s6). The number and size of the multicellular spheroids formed on
33
34 SMH-1, SMH-2 and SMH-3 were counted and measured (Supporting Information
35
36 Figure s7). Researches showed that the size and size distribution of multicellular
37
38 spheroids were cell-line dependent and the numbers of multicellular spheroids formed
39
40 increased with the density of adhering cells caused by partially exposed Fe_3O_4
41
42 nanoparticles^{12, 31}. Results showed that the size of multicellular spheroids formed on
43
44 different samples were of no significant difference. The numbers of multicellular
45
46 spheroids formed on sliced magnetic hydrogel per sample slightly increased when the
47
48
49
50
51
52
53
54
55
56
57
58
59
60

1
2
3
4 concentration of magnetic nanoparticles increased. Based on Figure 3a, the cell
5
6 adhesive area of sliced magnetic hydrogel increased from approximately 0.9% to 17%
7
8 when the concentration of magnetic nanoparticles rose from 0.05 mg/mL to 1.8
9
10 mg/mL and the density of adhesive site was still not large enough to prevent cells
11
12 from forming multicellular spheroids¹⁷. However, farther increasing the density of
13
14 magnetic nanoparticles will induce the aggregate and precipitate of nanoparticles
15
16 when mixed with the polymer monomer solution. This makes it not possible to
17
18 fabricate magnetic hydrogel containing higher concentration of magnetic
19
20 nanoparticles.
21
22
23
24

25
26 Considering the suitable concentration of magnetic nanoparticle was demanded for
27
28 alternating magnetic field induced hyperthermia of magnetic hydrogel³², we chose
29
30 SMH-2 for further evaluation. Results showed that GFP-293A cells overlaid as
31
32 single-cell suspension on SMH-2 formed 3D cell multicellular spheroids one day after
33
34 plating (Figure 4a) and the average diameter and total numbers of multicellular
35
36 spheroids clearly increased in 6 days post plating (Figure 4b), which was not observed
37
38 with the GFP-293A cells cultured in 24-well plates (Figure 4c). 3D reconstruction
39
40 images obtained with Laser confocal fluorescence microscope showed that
41
42 multicellular spheroids were not formed inside the sliced magnetic hydrogel but on
43
44 the surface (Supporting Information, S1 mov.). These multicellular spheroids won't
45
46 drop off when underwent a gentle shaking. To further investigate the formation
47
48 process of multicellular spheroids on the surface of sliced magnetic hydrogel, an
49
50 Olympus X- living cell workstation was used to acquire the time-lapse images of
51
52
53
54
55
56
57
58
59
60

1
2
3 seeded cells (cell seeding density was doubled to accelerate the spheroid formation)
4
5
6 every 20 min at 100 × magnification for 1 day (Supporting Information, S2 mov.).
7
8
9 Results demonstrated that GFP-293A cells initially formed small aggregates *via*
10
11 proliferation and migration, and then these aggregates further merged into irregular
12
13 spheroids and finally became mature with inerratic geometry (Figure 5). The
14
15 co-localization of magnetic nanoparticle assemblies and multicellular spheroids were
16
17 demonstrated with optical microscopy images at low exposure. Results showed that
18
19 GFP-293A cells started to aggregate 2 hours after seeding (Supporting Information
20
21 Figure s8). Intervals among assemblies were smaller than the size of single cell and
22
23 were able to be stepped over easily by cells. After two days, multicellular spheroids
24
25 had formed and localized on top of the nanoparticle assemblies. Since the diameter of
26
27 multicellular spheroids ranged in hundreds of micrometers, the optical microscope
28
29 could not focus on the surface of sliced magnetic hydrogel and multicellular spheroids
30
31 at the same time (Supporting Information Figure s9). After culturing for 6 days, with
32
33 the growing of those spheroids, they became opaque therefore the nanoparticle
34
35 assemblies underneath became invisible (Supporting Information Figure s10).
36
37 However, the assemblies around the multicellular spheroids proved that those areas
38
39 underneath spheroid certainly had assemblies exposed, owing to the
40
41 homo-distribution of assemblies that area with no assemblies surrounded by area with
42
43 assemblies does not possibly exist. The spontaneous formation process of
44
45 multicellular spheroids, cell morphology and behaviors were similar with cells culture
46
47 on staple commercial materials (such as Matrigel)³³, but costs of sliced magnetic
48
49
50
51
52
53
54
55
56
57
58
59
60

1
2
3
4 hydrogel were much lower and almost have no batch-to-batch discrepancy.

5
6 Furthermore, the spheroids formation efficiency of cells cultured on sliced magnetic
7
8 hydrogels was also no worse than those developed techniques³⁴.

9
10
11 Most fully-fledged techniques used to generate multicellular spheroids (such as
12
13 hanging drops) nowadays were designed based on the “non-adhesion” strategy.

14
15 Findings in these models demonstrated the spheroid formation capability among
16
17 different cell lines were obviously different. Researchers found that many tumor cell
18
19 lines could only form loose aggregates, an architecture that loses tight cell-cell

20
21 conjunction thereby significantly different from the *in vivo* tumor features³⁴. We chose
22
23 breast cancer cell line MCF-7 and ovarian cancer cell line SK-OV-3 as models to

24
25 study the multicellular spheroid formation capability on the sliced magnetic hydrogel.
26
27 Results showed that after 3 days culture, MCF-7 cells initially formed a large amount

28
29 of small cell aggregates (Figure 6a). These cell aggregates continued to grow and
30
31 merge to form multicellular spheroids after 6 days culture (Figure 6b). Results of

32
33 live/dead staining with Fluorescein diacetate (FDA) and Propidium Iodide (PI)
34
35 demonstrated that most dead cells were located in the center of partial multicellular

36
37 spheroids after 9 days culture (Figure 6c-d), which should be induced by the diffusion
38
39 limitation of nutrition and metabolic wastes. SK-OV-3 cells cultured on sliced

40
41 magnetic hydrogel presented similar results (Figure 5e-f), although dead cells (red)
42
43 were observed after cultured for 12 days (Figure 6g-h). The proliferation of tumor

44
45 cells in monolayer was comparably faster than those cultured in 3D¹⁰. Results showed
46
47 that proliferation rate of SK-OV-3 cultured on sliced magnetic hydrogel was clearly

48
49
50
51
52
53
54
55
56
57
58
59
60

1
2
3
4 higher than those cultured in monolayer (Supporting Information Figure s11), which
5
6 was close to the growth rate in vivo³⁵. However, when cultured in hanging drop
7
8 system SK-OV-3 cells could only form cell aggregates with no penetration resistance
9
10 (Supporting Information Figure s12). The drug resistance of SK-OV-3 cells cultured
11
12 on the sliced magnetic hydrogel and in the culture plates was preliminarily evaluated
13
14 with doxorubicin as model drug. Results demonstrated that the cells cultured on sliced
15
16 magnetic hydrogel presented stronger drug resistance than those cultured on plates
17
18 when the concentration of doxorubicin increased to 100 $\mu\text{g}/\text{ml}$ after culturing for 9
19
20 days, which was due to the compact structures of multicellular spheroids (Supporting
21
22 Information Figure s13). Previous studies showed that SK-OV-3 cells could form
23
24 multicellular spheroids and showed drug resistance when cultured inside
25
26 RGD-modified, cell-secreted metalloproteinases (MMP) sensitive hydrogel¹⁰.
27
28 Furthermore, researches demonstrated that adding extracellular adhesion molecules
29
30 (fibronectin, laminin or reconstituted basement membrane) into the hanging drop
31
32 culture system could induce SK-OV-3 cells to form multicellular spheroids³⁶.
33
34 Combined with our findings, we speculate that the matrix with appropriate
35
36 cell-adhesion properties were necessary for the formation of multicellular spheroid³⁷.
37
38 Further studies on the cytobiology mechanism of spheroid formation could be carried
39
40 on by applying this composite material as platform.
41
42
43
44
45
46
47
48
49
50
51
52
53
54

55 4. CONCLUSION

56 In summary, a novel sliced magnetic hydrogel with certain regularity and
57
58
59
60

1
2
3
4 reproducibility was prepared and applied as 3D cell culture platform. By combining
5
6 anti cell-adhesive hydrogel and cell-adhesive magnetic colloidal assemblies together,
7
8 this composite material provided a matrix with cell-adhesive microarray on the
9
10 surface which could enhance the cell- cell interaction. Cells from different cell lines
11
12 could spontaneously form multicellular spheroids when cultured on this
13
14 functionalized interface, and on this platform cells which could only form cell
15
16 aggregates in traditional 3D cell culture system were able to form multicellular
17
18 spheroids, which promote the applicability of this matrix. This low-cost magnetic
19
20 hydrogel will have a great potential in *in vitro* evaluation of hyperthermia and
21
22 chemotherapy or cytobiology researches.
23
24
25
26
27
28
29
30

31 ■ ASSOCIATED CONTENT

32 * S Supporting Information

33
34
35
36 The morphology and magnetic properties of $\text{Fe}_3\text{O}_4@\text{PSC}$ MNPs, the optical microscope
37
38 images of side view of sliced magnetic hydrogel and sectional view of sliced
39
40 magnetic hydrogel with different slicing depth, AFM characterization of sliced
41
42 magnetic hydrogel, Statistical diagram of numbers and size of multicellular spheroids
43
44 formed on SMH-1, SMH-2 and SMH-3, morphology of GFP-293A cells cultured on
45
46 sliced disorganized magnetic hydrogel, SMH-1 and SMH-3, morphology of SK-OV-3
47
48 cells cultured in hanging drop system, 3D reconstruction images obtained with Laser
49
50 confocal fluorescence microscope and time lapsed video of GFP-293A cells cultured
51
52 on SMH-2.
53
54
55
56
57
58
59
60

■ AUTHOR INFORMATION

Corresponding Authors

*E-mail: zhangtianshu@seu.edu.cn(T.Z.) Fax: +86 25 83272460.

*E-mail: guning@seu.edu.cn(N.G.) Fax: +86 25 83272460.

Author Contributions

† These two authors contributed equally in this manuscript. All authors have given approval to the final version of the manuscript.

Notes

The authors declare no competing financial interest.

■ ACKNOWLEDGMENTS

We acknowledge the support of National Natural Science Foundation of China (61127002, 61420106012). T. Z. Zhang is grateful for supports from the program for New Century Excellent Talents in University (NCET-09-0298) and Suzhou medical apparatus and new medicine Fund (ZXY201440), and J. F. Sun is thankful for supports from National Natural Science Foundation of China (NSFC, 21273002). K.Hu. is also grateful for supports from the research innovation plan of colleges and universities postgraduates of Jiangsu Province (CXLX12_0120).

■ REFERENCES

- (1) Cukierman, E.; Pankov, R.; Stevens, D.R.; Yamada, K.M. Taking Cell-Matrix Adhesions to the Third Dimension. *Science* **2001**, 294(5547), 1708–1713.

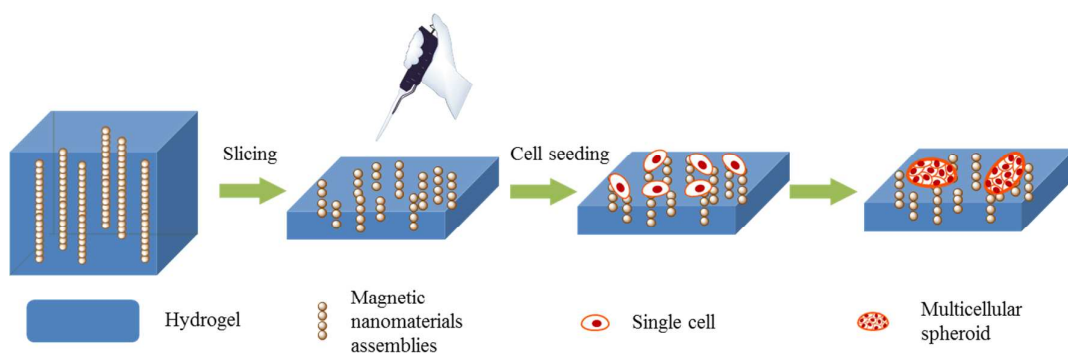
- 1
2
3
4 (2) Even-Ram, S.; Yamada, K.M. Cell Migration in 3D Matrix. *Curr. Opin. Cell Biol.*
5
6 **2005**, 17, 524–532.
7
8
9 (3) Tibbitt, M.W.; Anseth, K.S. Hydrogels as Extracellular Matrix Mimics for 3D Cell
10
11 Culture. *Biotechnol. Bioeng.* **2009**, 103, 655–663.
12
13
14 (4) Fitzgerald, K.A.; Malhotra, M.; Curtin, C.M.; O' Brien, F.J.; O' Driscoll, C.M. Life
15
16 in 3D is Never Flat: 3D Models to Optimize Drug Delivery. *J. Control Release*
17
18 **2015**, 215, 29–54.
19
20
21 (5) Nyga, A.; Cheema, U.; Loizidou, M.; 3D Tumour Models: Novel *In Vitro*
22
23 Approaches to Cancer Studies. *J. Cell Commun. Signal.* **2011**, 5, 239–5248.
24
25
26 (6) Kraehenbuehl, T.P.; Langer, R.; Ferreira, L.S. Three-Dimensional Biomaterials for
27
28 the Study of Human Pluripotent Stem Cells. *Nat.Methods* **2011**, 8, 731–736.
29
30
31 (7) Zhang, P., Wang, S. Designing Fractal Nanostructured Biointerfaces for
32
33 Biomedical Applications. *Chemphyschem* **2014**, 15, 1550–1561.
34
35
36 (8) Sun, K.; Liu, H.; Wang, S.; Jiang, L. Cytophilic/Cytophobic Design of
37
38 Nanomaterials at Biointerfaces. *Small* **2013**, 9, 1444–1448.
39
40
41 (9) Liu, X.; Wang S. Three-dimensional Nano-biointerface as a New Platform for
42
43 Guiding Cell Fate. *Chem. Soc. Rev.* **2014**, 43, 2385–2401.
44
45
46 (10) Loessner, D.; Stok, K.S.; Lutolf, M.P.; Hutmacher, D.W.; Clements, J.A.; Rizzi,
47
48 S.C. Bioengineered 3D Platform to Explore Cell–ECM Interactions and Drug
49
50 Resistance of Epithelial Ovarian Cancer Cells. *Biomaterials* **2010**, 31, 8494–8506.
51
52
53 (11) Ziqi, Z.; Jianjun, G.; Yening, Z.; Ying, G.; Zhu, X. X.; Yongjun, Z. Hydrogel
54
55 Thin Film with Swelling-induced Wrinkling Patterns for High-throughput
56
57
58
59
60

- 1
2
3
4 Generation of Multicellular Spheroids. *Biomacromolecules* **2014**, 15, 3306–3312.
5
6 (12) Yukie, Y.; Atsuo, W.; Kaori, Y.; Anna, K.; Maki, K.; Hideo, N.; Yusei, K.; Yasushi,
7
8 K.; Hiroshi, Y.; Takako, F.; Tatsuya, A.; Hidehiko, O.; Juri, G.G.; Yasuhisa, F. The
9
10 Use of Nanoimprinted Scaffolds as 3d Culture Models to Facilitate Spontaneous
11
12 Tumor Cell Migration and Well-regulated Spheroid Formation. *Biomaterials* **2011**,
13
14 32, 6052–6058.
15
16
17
18 (13) Rizvi, I.; Celli, J.P.; Evans, C.L.; Abu-Yousif, A.O.; Muzikansky, A.; Pogue,
19
20 B.W.; Finkelstein, D.; Hasan, T.; Synergistic Enhancement of Carboplatin
21
22 Efficacy with Photodynamic Therapy in a Three-Dimensional Model for
23
24 Micrometastatic Ovarian Cancer. *Cancer Res.* **2010**, 70(22), 9319–9328.
25
26
27
28 (14) Engler, A.; Bacakova, L.; Newman, C.; Hategen, A.; Griffin, M.; Discher, D.
29
30 Substrate Compliance versus Ligand Density in Cell on Gel Responses. *Biophys.*
31
32 *J.* **2004**, 86(1), 617–628.
33
34
35
36 (15) Douezan, S.; Dumond J.; Brochard-Wyart F. Wetting transitions of cellular
37
38 aggregates induced by substrate rigidity. *Soft Matter* **2012**, 8 (17), 4578–483.
39
40
41 (16) Ryan, P.L.; Foty, R.A.; Kohn, J.; Steinberg, M.S. Tissue Spreading on
42
43 Implantable Substrates is a Competitive Outcome of Cell–Cell vs.
44
45 Cell–Substratum Adhesivity. *Proc. Natl. Acad. Sci. U.S.A.* **2001**, 98, 4323–4327.
46
47
48 (17) Powers, M. J.; Rodriguez, R. E.; Griffith, L.G. Cell-substratum Adhesion
49
50 Strength as a Determinant of Hepatocyte Aggregate Morphology. *Biotechnol.*
51
52 *Bioeng.* **1997**, 53(4), 415–426.
53
54
55
56 (18) Dvir, T.; Timko, B.P.; Brigham, M.D.; Naik, S.R.; Karajanagi, S.S.; Levy, O.; Jin,
57
58
59
60

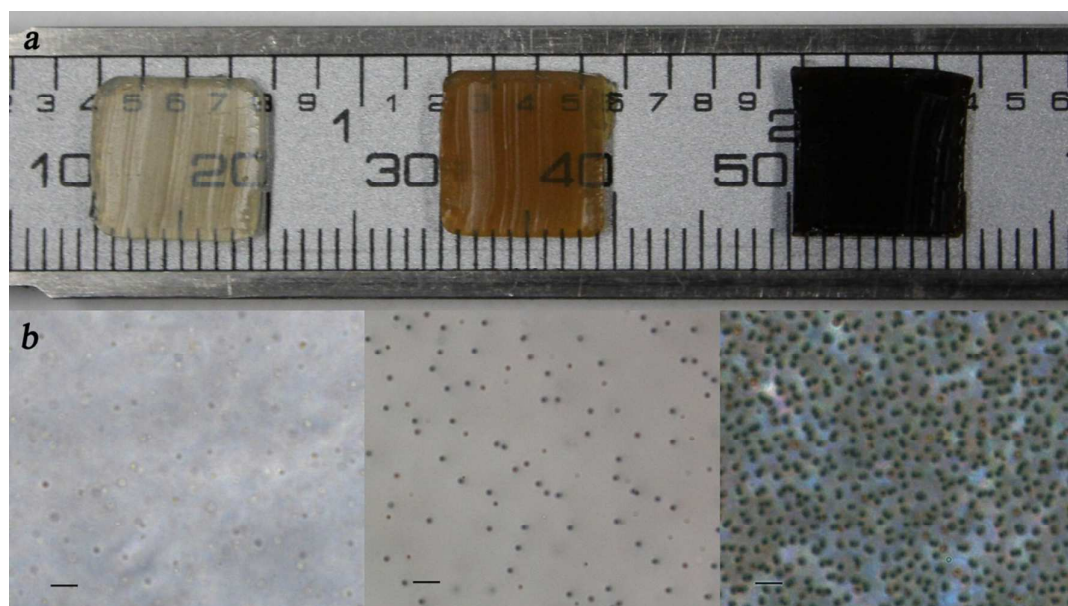
- 1
2
3
4 H.; Parker, K.K.; Langer, R.; Kohane, D.S. Nanowired Three-Dimensional
5
6 Cardiac Patches. *Nat. Nanotech.* **2011**, 6, 720–725.
7
8
9 (19) Ding, X.; Liu, H.; Fan, Y. Graphene-Based Materials in Regenerative Medicine.
10
11 *Adv. Healthcare Mater.* **2015**, 4, 1451–1468.
12
13 (20) Ayala, R.; Zhang, C.; Yang, D.; Hwang, Y.; Aung, A.; Shroff, S.S.; Arce, F.T.; Lal,
14
15 R.; Arya, G.; Varghese, S. Engineering the Cell-Material Interface for Controlling
16
17 Stem Cell Adhesion, Migration, And Differentiation. *Biomaterials* **2011**, 32,
18
19 3700–3711.
20
21
22 (21) Hu, K.; Sun, J.; Guo, Z.; Wang, P.; Chen, Q.; Ma, M.; Gu, N. A Novel Magnetic
23
24 Hydrogel with Aligned Magnetic Colloidal Assemblies Showing Controllable
25
26 Enhancement of Magnetothermal Effect in the Presence of Alternating Magnetic
27
28 Field. *Adv. Mater.* **2015**, 27, 2507–2514.
29
30
31 (22) Weinstein, J.S.; Varallyay, C.G.; Dosa, E.; Gahramanov, S.; Hamilton, B.;
32
33 Rooney, W.D.; Muldoon, L.L.; Neuwelt, E.A. Superparamagnetic Iron Oxide
34
35 Nanoparticles: Diagnostic Magnetic Resonance Imaging and potential Therapeutic
36
37 Applications in Neurooncology and Central Nervous System Inflammatory
38
39 Pathologies, a Review. *J. Cereb. Blood Flow Metab.* **2010**, 30, 15–35.
40
41
42 (23) Xia, Y.; Nguyen, T.; Yang, M.; Lee, B.; Santos, A.; Podsiadlo, P.; Tang, Z.;
43
44 Glotzer, S. C.; Kotov N. A. Self Assembly of Self-Limiting, Monodisperse
45
46 Supraparticles from Polydisperse Nanoparticles. *Nat. Nanotech.* **2011**, 6, 580–587.
47
48
49 (24) Cao, B.; Li, Z.; Peng, R.; Ding, J. Effects of Cell-Cell Contact and Oxygen
50
51 Tension on Chondrogenic Differentiation of Stem Cells. *Biomaterials* **2015**, 64,
52
53
54
55
56
57
58
59
60

- 1
2
3
4 21–32.
5
6 (25) Feng, Z. Q.; Chu, X. H.; Huang, N. P.; Wang, T.; Wang, Y. C.; Shi, X. L.; Ding, Y.
7
8 T.; Gu, Z. Z. The Effect of Nanofibrous Galactosylated Chitosan Scaffolds on the
9
10 Formation of Rat Primary Hepatocyte Aggregates and the Maintenance of Liver
11
12 Function. *Biomaterials* **2009**, 30, 2753–2763.
13
14
15
16 (26) Wang, D. D.; Cheng, D.; Guan, Y.; Zhang, Y. J. Thermoreversible Hydrogel for
17
18 In Situ Generation and Release of HepG2 Spheroids. *Biomacromolecules* **2011**, 12,
19
20 578–584.
21
22
23
24 (27) Gallagher, J.O., Mcghee, K.F., Wilkinson, C.D.W.; Riehle, M.O. Interaction of
25
26 Animal Cells with Ordered Nano-Topography. *IEEE T. Nanobiosci.* **2002**, 3,
27
28 24–28.
29
30
31 (28) Kunzler, T. P.; Tanja, D.; Martin, S.; Spencer, N. D. Systematic Study of
32
33 Osteoblast and Fibroblast Response to Roughness by Means of
34
35 Surface-morphology Gradients. *Biomaterials* **2007**, 28, 2175–2182.
36
37
38
39 (29) Hacking, S. A.; Tanzer MHarvey, E. J.; Krygier, J. J.; Bobyn, J. D. Relative
40
41 Contributions of Chemistry and Topography to the Osseointegration of
42
43 Hydroxyapatite Coatings. *Clin. Orthop. Relat. R.* **2002**, 405, 24–38.
44
45
46
47 (30) Hallab, N.; Bundy, K. K.; Moses, R.; Jacobs, J. Evaluation of Metallic and
48
49 Polymeric Biomaterial Surface Energy and Surface Roughness Characteristics for
50
51 Directed Cell Adhesion. *Tissue Eng.* **2001**, 7, 55–71.
52
53
54 (31) Kunz-Schughart, L.A.; Freyer, J.P.; Hofstaedter, F.; Ebner, R.; The Use of 3-D
55
56 Cultures for High-throughput Screening: the Multicellular Spheroid Model. *J.*
57
58
59
60

- 1
2
3
4 *Biomol. Screen.* **2004**, 9, 273–285.
- 5
6 (32) Xu, R.; Zhang, Y.; Ma, M.; Xia, J.; Liu, J.; Guo, Q.; Gu, N. Measurement of
7
8 Apecific Absorption Rate and Thermal Simulation for Arterial Embolization
9
10 Hyperthermia in the Maghemite-gelled Model. *IEEE T. Magn.* **2007**, 43,
11
12 1078–1085.
- 13
14
15 (33) Celli, J.P.; Rizvi, I.; Evans, C.L.; Abu-Yousif, A.O.; Hasan, T. Quantitative
16
17 Imaging Reveals Heterogeneous Growth Dynamics and Treatment-dependent
18
19 Residual Tumor Distributions in a Three-dimensional Ovarian Cancer Model. *J.*
20
21 *Biomed. Opt.* **2010**, 15, 1–10.
- 22
23
24 (34) Ivascu, A.; Kubbies, M. Rapid Generation of Single-Tumor Spheroids for
25
26 High-Throughput Cell Function and Toxicity Analysis. *J. Biomol. Screen.* **2006**, 11,
27
28 922–932.
- 29
30
31 (35) Cukierman, E.; Pankov, R.; Yamada, K. M. Cell interactions with
32
33 three-dimensional matrices. *Curr. Opin. Cell Biol.* **2015**, 14, 633–639.
- 34
35
36 (36) Sodek, K.L.; Ringuette, M.J.; Brown, T.J. Compact Spheroid Formation by
37
38 Ovarian Cancer Cells is Associated with Contractile Behavior and an Invasive
39
40 Phenotype. *Int. J. Cancer* **2009**, 124, 2060–2070.
- 41
42
43 (37) Guo, Z.; Hu, K.; Sun, J.; Zhang, T.; Zhang, Q.; Song, L.; Zhang, X.; Gu, N.
44
45 Fabrication of Hydrogel with Cell Adhesive Micropatterns for Mimicking the
46
47 Oriented Tumor-Associated Extracellular Matrix. *ACS Appl. Mater. Interfaces*
48
49 **2014**, 6, 10963–10968.
- 50
51
52
53
54
55
56
57
58
59
60



17 **Figure 1.** Schematic show of sliced magnetic hydrogel applied as 3D cell culture matrix.



40 **Figure 2.** Photographs (a) and optical microscope images (b) of sliced magnetic hydrogel samples SMH-1, SMH-2 and SMH-3 (from the left to the right). Scale bar in (b): 10 μm .

41
42
43
44
45
46
47
48
49
50
51
52
53
54
55
56
57
58
59
60

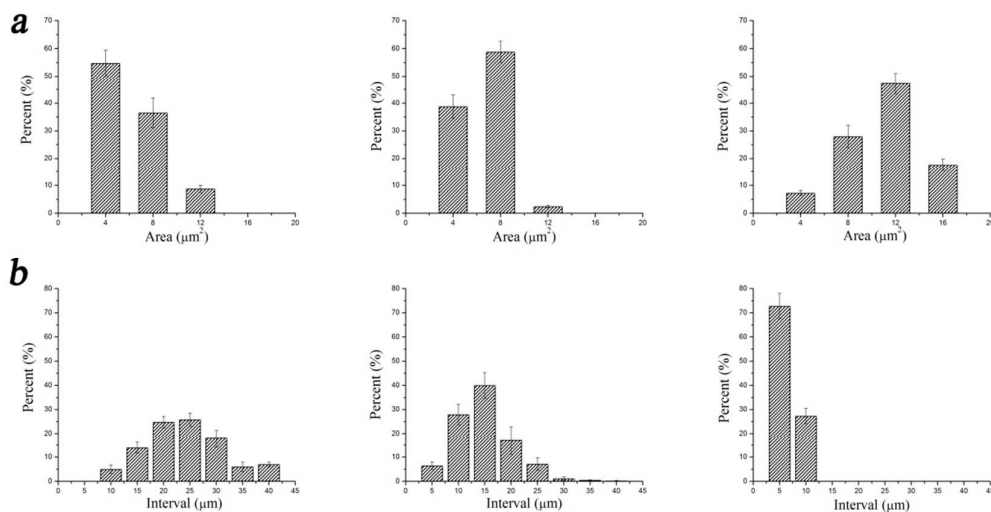


Figure 3. Statistical diagrams of assembly sectional area (a) and intervals between magnetic nanoparticle assemblies (b) of sliced magnetic hydrogel samples SMH-1, SMH-2 and SMH-3 (from the left to the right).

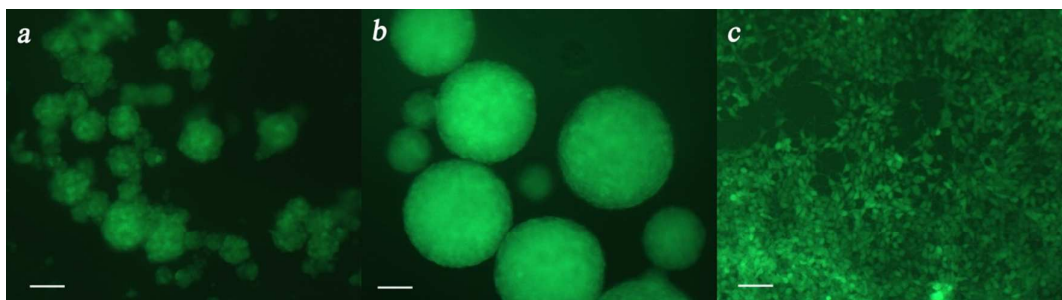
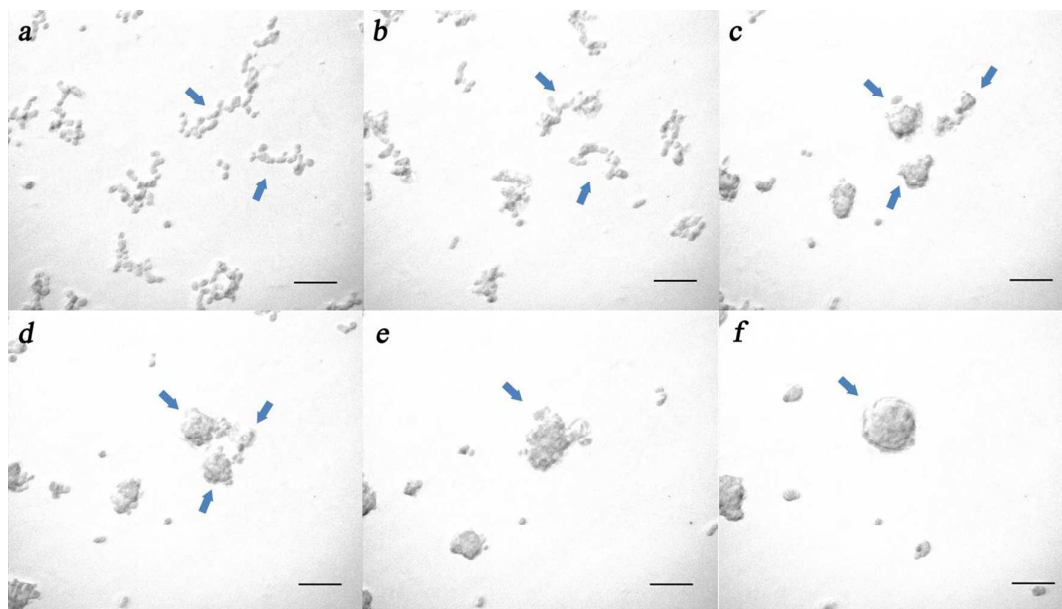
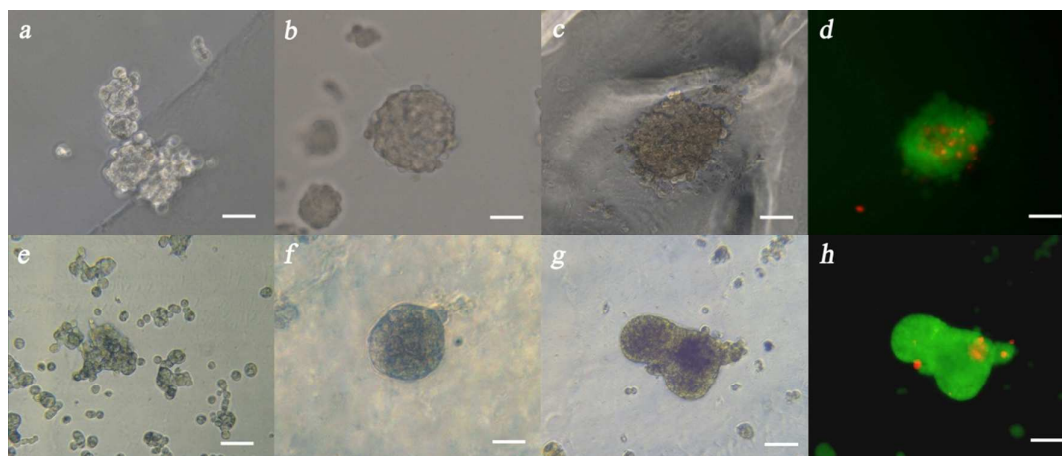


Figure 4. Florescent microscope image of GFA-293A cells cultured on sliced magnetic hydrogel sample SMH-2 for 1 day (a) and 6 days (b) and on 24-well plate for 6 days (c). Scale bar: 100 μm .



23
24
25
26
27

Figure 5. (a-f) time lapse microscope images of GFP-293A cells cultured on sliced magnetic hydrogel. Blue arrows point the spontaneous formation process of multicellular spheroids via migration, proliferation and mergence. Scale bar: 100 μm .



44
45
46
47
48
49
50
51
52
53
54
55
56
57
58
59
60

Figure 6. Optical microscope images of MCF-7 cells and SK-OV-3 cells cultured on sliced magnetic hydrogel for 3 (a & e), 6 (b & f), 9 (c) and 12 (g) days. Live/dead cells were stained with PDA (green)/PI (red) (d & h). Scale bar: 50 μm .

1
2
3
4
5
6
7
8
9
10
11
12
13
14
15
16
17
18
19
20
21
22
23
24
25
26
27
28
29
30
31
32
33
34
35
36
37
38
39
40
41
42
43